

MODELING OF GAS JET DISTRIBUTION IN POROUS ENVIRONMENT

Michael Michaylov

University of Mining and Geology St. Ivan Rilski
 Sofia, 1700 Bulgaria

ABSTRACT

Preventive and operative nitrogen injection against spontaneous combustion of coal in gob areas is the most expensive technology of prevention and extinguishing sponcom fires employed in modern underground coalmines. However, this method does not always produce the desired preventive and quenching effect due to insufficient data on nitrogen jet distribution in porous environment and on the basic gas-air flow in inaccessible gob areas. Efficiency and optimization analysis of nitrogen injection parameters requires new knowledge about the process of inert gas distribution in above described conditions – porous environment in a rectangular area with two solid and two porous boundaries; basic flow, aerodynamic reversal of basic and injected flows. The paper presents a physico-mathematical model of gas jet semi-restricted by the coal seam that flows out and disseminates together with the basic flow. Model solution provides assessment of interaction among porous environment parameters, injection and basic flows all of which in turn allow evaluation of jet parameters.

INTRODUCTION TO PROBLEM

Gas environment inertization in gob areas for the purpose of reducing natural methane release [1,5], has restricted impact on small sections therein. Nitrogen injection in the porous gob environment has been widely employed during the last fifteen years [2,6] in mining of coal seams highly prone to spontaneous combustion. The strictly empirical approach to justification of nitrogen inertization prevails both in world and Bulgarian mining practice. Such approach does not allow prediction of necessary nitrogen quantities for gob inertization because no surveys are available on injection sites, on the way nitrogen flows and disseminates, on the efficiency of application or on the relationship of all those factors with methane release in gob areas. Lack of research results and engineering tools is particularly strongly felt whilst employing the method for sponcom fire prevention. A comprehensive picture of nitrogen utilization dynamics in Babino Mine could be obtained from the data shown on fig.1. There is a nearly functional relationship between nitrogen consumption and monthly coal production. Increase of monthly production from 20000 to 45000 t results in reduction of nitrogen consumption per t coal produced by 2.5 times. (fig.1b). Power cost is the dominating element in the production cost of $1 Nm^3$ nitrogen, the latter being slightly lower than the cost of 1 kWh electricity.

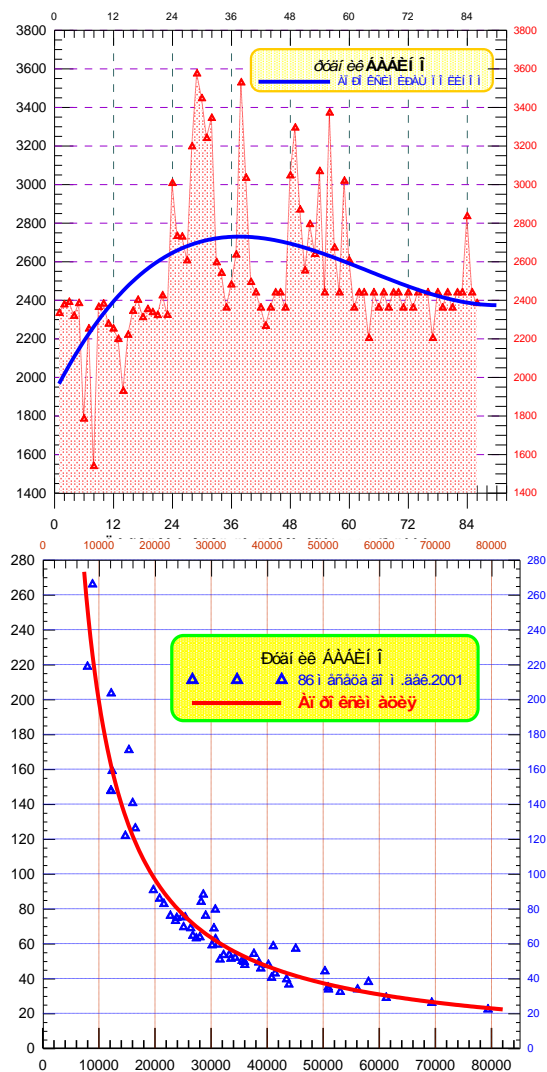
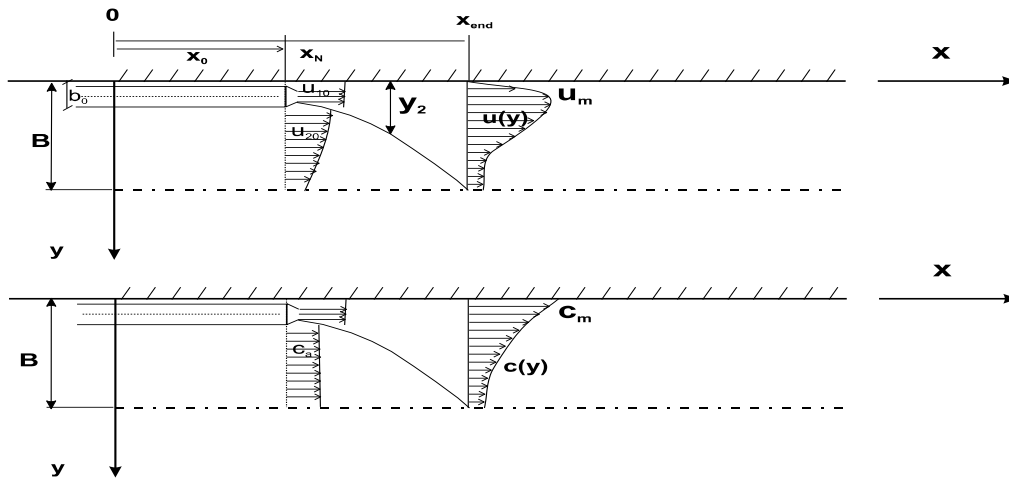


Figure 1. Nitrogen inertization parameters in Babino Mine



West - gob porous boundary $X=0, Y \in (0..B)$ Y_2 - jet expansion X_0 - nitrogen flow
 North-pillar of intane gallery $Y=0, X \in (X_0..X_N)$ U_m - maximal velocity b_0 - injector size

Figure 2. Physic al model of nitrogen jet distribution

Nitrogen distribution in porous gob environment and in the main methane-air flow is a complex aerodynamic problem. Its physical nature requires modeling in two zones with different energy characteristics – a jet zone wherein the nitrogen jet preserves its identity and a flow zone wherein the nitrogen mixes with the main flow and continues to disseminate as a flow and not as a jet. [1]. Jet zone end is the initial boundary of the flow zone representing the natural interaction between the two. [2].

FLOW MODEL

Physico-mathematical model formulation is based on the interaction of semi-restricted flat nitrogen jet (fig.2) and the main filtration air flow, and used for solving specific engineering tasks in specific conditions.. There are big contrasts between mechanical energies of air and nitrogen flows. The differences in internal energies of the two flows are insignificant. In the initial section of the nitrogen jet, air infusion is very small and concentrated in a narrow area around external jet boundary. This is due to the higher pressure inside the jet as compared to external porous enviroment.

Scale ratio of N- jet and its mixing with main flow allows investigation to concentrate on the main section of jet flow. The initial section can be ignored because of its small length. The flow can be described by the main conservation laws: of mass flow, of momentum, of kinetic energy, and of admixture mass. These equations are, as follows (for N-jet on fig.2):

$$\int_0^{y_2} u dy + \int_{y_2}^B u_2 dy = b_0 u_{10} + (1 - k_1 X)(B - b_0) u_{20} \quad (1)$$

$$\rho \int_0^{y_2} u^2 dy + \rho \beta \int_{y_2}^B u_2^2 dy + \int_0^{y_2} (p - p_2) dy = \rho b_0 u_{10}^2 + \quad (2)$$

$$\rho(B - b_0)(1 - k_1 X)u_{20}u_{20} - \tau_0 X - \xi_m \frac{\rho}{2} \int_0^{y_2} u^2 dy$$

$$\frac{\partial}{\partial X} \left[\int_0^{y_2} \rho_g u(u - u_2)^2 dy + 2a \int_0^{y_2} (u - u_2) p dy \right] = \quad (3)$$

$$-2 \int_0^{y_2} \rho_g v_{tg} \left[\frac{\partial u}{\partial y} \right]^2 dy - \frac{\rho}{2} \int_0^{y_2} \xi_m u^3 dy$$

$$\frac{\partial}{\partial X} \int_0^{y_2} (\rho_g v_{tg} u) dy = 0 \quad (4)$$

Hydraulic jet pressure and energy losses in (2) and (3) are described by the following expressions:

$$\Delta p = \xi_m \frac{\rho}{2} u^2; \quad E_1 = \Delta p u = \xi_m \frac{\rho}{2} u^3$$

Local resistance factor of the porous environment is calculated, as follows:

$$\left| \begin{aligned} \frac{\partial p}{\partial X} &= \xi_m \frac{\rho u^2}{2} \\ \frac{\partial p}{\partial X} &= a_x \rho v u + \beta_x \rho u^2 = \rho u (a_x v + \beta_x u) \end{aligned} \right. \quad (5a)$$

On equalization of the right sides and subsequent division by ρu , the following expression is obtained for the local resistance factor of the porous environment:

$$\xi_m = \left(\frac{a_x v}{u} + \beta_x \right) \quad (5)$$

where: α_x and β_x are the coefficients respectively of viscous and inertial resistance of porous environment [1], increasing with gob depth.

For crosswise distribution of velocity profiles along jet flow, two similarity functions are taken in the equation system:

- For wall-adjacent boundary layer [3]:

$$f' = \xi^{1/N} \tag{6}$$

where $f' = u/u_{20}$, respectively $f' = u/u_m$, $N = f(\text{Re})$

The model accepts $N=9$.

- For jet boundary layer [4]:

$$f = f(\eta) = 1 - 3\eta^2 + 2\eta^3 \tag{7}$$

where: $\eta = \frac{y - y_m}{y_2 - y_m}$

Jet kinetic energy equation (3) velocity distribution follows Abramovich [7]:

$$\frac{u}{u_m} = 1.48 \xi^{1/7} [1 - \text{erf}(0.68\xi)] = f_1 \tag{7}$$

where: $\xi = y/y_2$

Jet outflow into porous environment allows the assumption that crosswise pressure distribution follows a model similar to velocity distribution one (6):

$$\frac{p_{\max} - p}{p_{\max} - p_2} = f(p) = 1 - 3\xi^2 + 2\xi^3 \tag{8}$$

Velocity similarity function in hydro-dynamic boundary layer:

$$f_1 = 1.48 \xi^{1/7} [1 - \text{erf}(0.68\xi)] \tag{7a}$$

after transformation and sensitivity analysis gives the expression:

$$f_1 = 1.48 \xi^{1/7} - 1.136 \xi^{8/7} + 0.175 \xi^{29/7} - 0.0243 \xi^{36/7} \tag{7b}$$

which defines the velocity profile shown on fig.3.

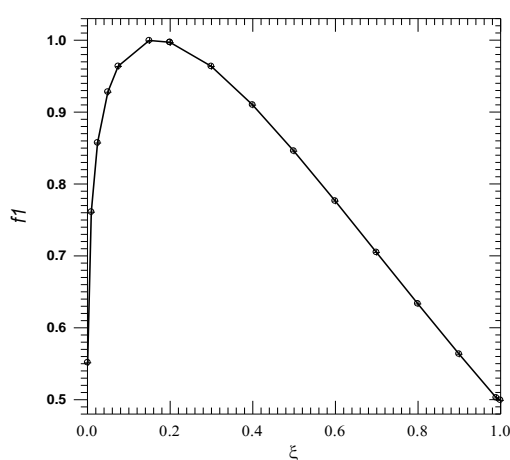


Figure 3

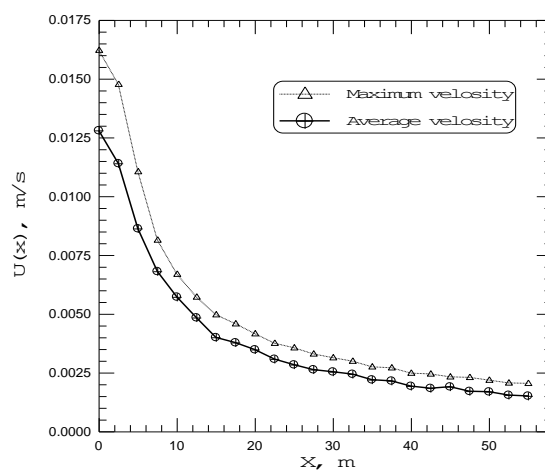


Figure 4

With accepted similarity of crosswise velocity and pressure distribution, the equations 2-5 are solved. Second integrals in (1) and (3) are solved using approximation of the solution for air leak velocity distribution in the zone $x \in (0,70)$, $y \in (0,15)$, obtained on the main flow model [5]. Average and maximum velocity profiles are shown on fig.4, whereof characteristic factors in (2) and (3) have values, as follows:

- Boussineq factor $\beta = \bar{u}_2 / u_{2\max} = 0.64$;
- Coriolis factor $\beta = \bar{u}_2^2 / u_{2\max}^2 = 0.8$.

After transformation of the four (2-5) integral equations, the following system results:

$$A_{11} \bar{y}_2 \bar{u}_m + A_{12} \bar{y}_2 = A_{13} \tag{9}$$

$$A_{21} \bar{y}_2 \bar{u}_m^2 + A_{22} \bar{y}_2 \bar{u}_m + A_{23} \bar{y}_2 \Delta p + A_{24} \bar{y}_2 = A_{25} \tag{10}$$

$$\frac{d}{dx} [A_{31} \bar{y}_2 \bar{u}_m^3 + A_{32} \bar{y}_2 \bar{u}_m \Delta p] + A_{33} \bar{y}_2 \bar{u}_m^2 + A_{34} \bar{y}_2 \bar{u}_m + A_{35} \bar{y}_2 \bar{u}_m^3 = 0 \tag{11}$$

$$\bar{y}_2 \bar{u}_m \bar{s}_m = A_{41} \tag{12}$$

where dimensionless values are unknown:

- ♦ Maximal velocity of main N-jet - $\bar{u}_m = u_m / u_{10}$
- ♦ Jet width - $\bar{y}_2 = y_2 / B$

- ♦ Maximal pressure difference - $\Delta p = \frac{P_m - P_2(x)}{\rho u_{10}^2}$

- ♦ Maximal nitrogen concentration - $\bar{s}_m(x)$,

Valid for any cross section of the jet flow along X. Coefficients A_{ij} and integrals φ_{mn} therein are given in the denotation list.

Equations 9-12 are of different types and direct solution of the system is not possible. Moreover, the third equation is a differential one in respect of Δp . The equation system (9-12) is solved by consecutive iterations in respect of unknown parameters and alternating exchange of unknown values with approximate values resulting from previous iterations/equations. First, we express \bar{y}_2 from (9) and substitute the resulting expression including \bar{u}_m , in (10). The latter is solved as a square power equation in respect to \bar{u}_m and thus its first approximation is obtained. The approximate

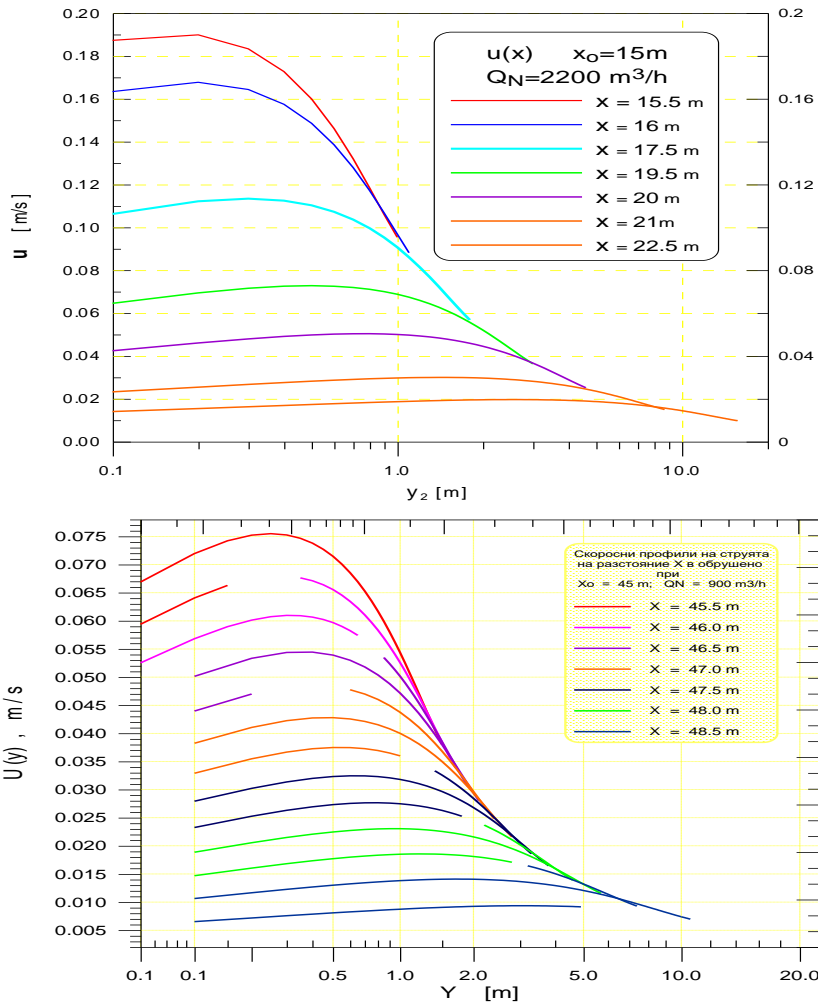


Figure 5. Velocity profiles during N-injection of Q_N at depth X_0

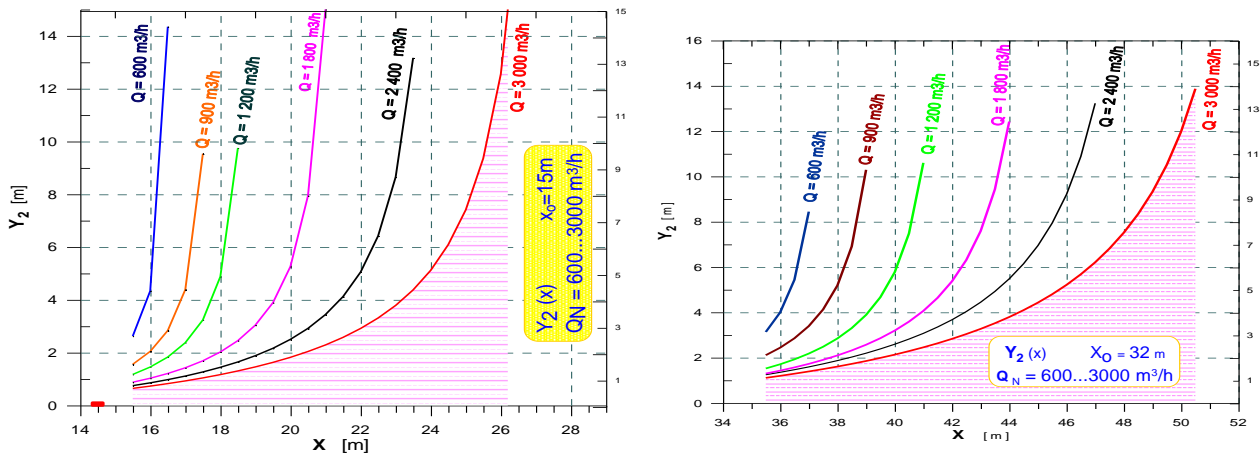


Figure 6. N-jet expansion Y_2 during injection of Q_N at depth X_0

values of \bar{u}_m and \bar{y}_2 are substituted in (11) and this is numerically solved for Δp . Resulting values are substituted back in source equations and the procedure is repeated until the required accuracy for \bar{u}_m is achieved. The solution of (9-

12) follows flow direction in steps of $st \bar{x} = 1$ until the set expansion zone $y_2 = B$ is achieved by means of NitroJet software [6].

EXPERIMENTAL RESULTS

Numerical experiments were carried out for retreat longwall face. Face length is $L_f = 100m$, extracted seam thickness is $m = 3m$. Ventilation air flow is $Q_f = 8 m^3/s$ with methane concentration $C_{in} = 0.2\%$. Of this flow, $Q_l = 0.892 m^3/s$ leak into the gob. Methane of $Q_m = 0.06 m^3/s$ is released in the gob and carried out by air leakages ($Q_l + Q_m$) in the tailgate section of the face. Gob resistance varies as described in [1].

At these initial modeling conditions, variation of N-jet parameters is studied with injection rates Q_N from $600 m^3/h$ to $3000 m^3/h$, at six-level variation (0.17, 0.25, 0.33, 0.5, 0.61 и $0.83m^3/s$); and injection into the gob along intake road at depths of x_N (fig.1) 15m, 25m, 35m и 45m .

The wide variation range of injection parameters was chosen to obtain general conclusions and trends for N-jet distribution [2,6]. Within the framework of research [6], some results whereof are presented herein, 24 variants were solved in the above-shown variation range for x_N and Q_N . Some modeling results are shown on fig. 5 – fig.8.

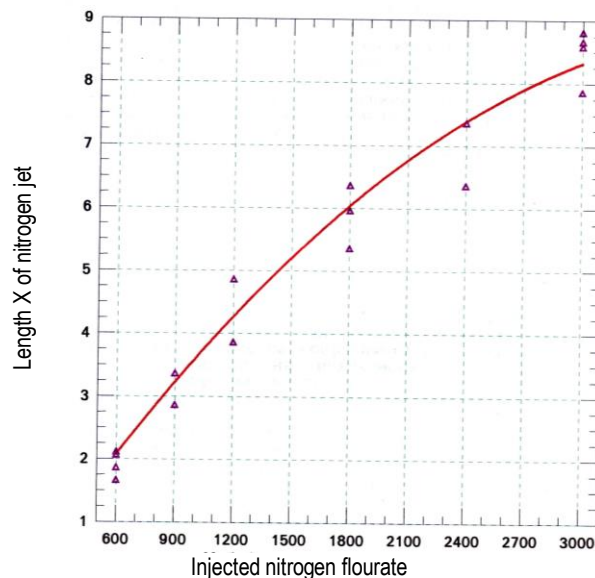


Figure 8. Nitrogen jet length

DISCUSSION

Research of nitrogen jet distribution in porous environment should provide answers to the following important issues:

- ⇒ Variation of main hydrodynamic parameters – velocity and expansion of jet flow; impact of variable porous characteristics, of main airflow and its initial velocity, on the resultant jet flow;
- ⇒ Distributions of nitrogen jet velocity and concentration at jet section end. These distributions are boundary conditions for investigation of N-jet impact in the remaining larger gob portion;
- ⇒ Efficiency of inertization with the method presently employed. The negative answer to this issue would require looking for alternative decisions in order to optimize technology including decisions that allow combined use of other methods for prevention and extinguishing of sponcom gob fires.

Variation of main hydrodynamic jet flow parameters . In the above-resolved variants, nitrogen flow is 18.4% to 93.5% of air leakage flow into gob area. Initial N-jet outflow velocity at injection tube end varies from 21 m/s to 106 m/s. Immediately after leaving the pipe, the jet hits the porous environment at a height of 1 m from gob floor and the velocity is sharply reduced whilst expanding in width and height. Numerical experiments show leap-wise expansion until the first 5 injector diameters ($5b_0$) in flow direction

Jet expansion along gob height (z) takes place a lot faster that along gob area because of the resistance around the intake gate pillar ($y=0$ on fig.1). On completion of expansion in height, maximal velocity is reduced to 7...35 m/s, for injected quantities of Q_{N_2} . This reduction is accompanied by significant and fast increase of static pressure thus making injection of large nitrogen quantities near the face inefficient. This inefficiency involves premature outflow of injected

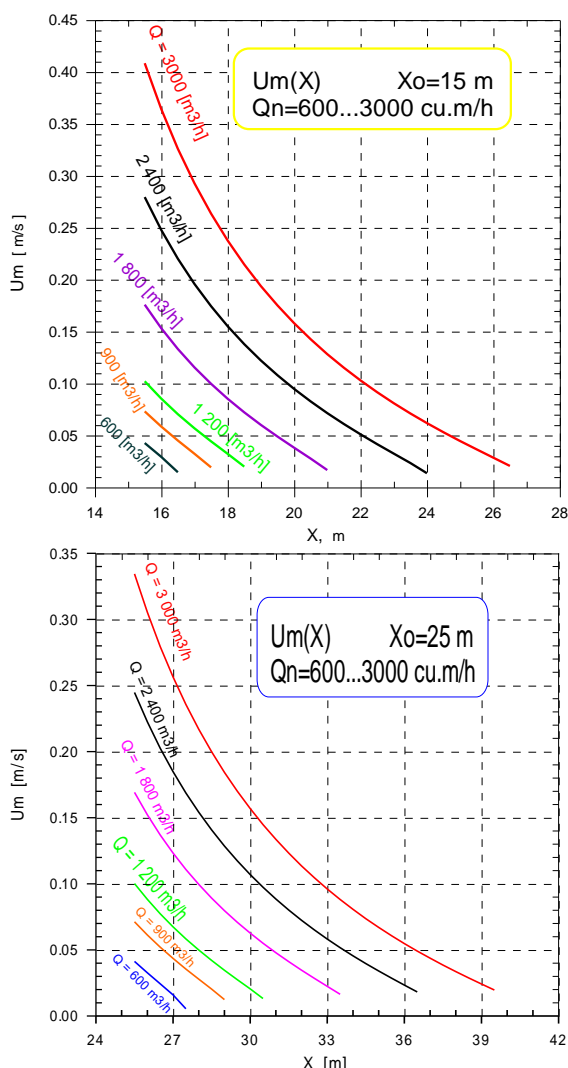


Figure 7. Maximal jet velocity variation

nitrogen from the gob before the atmosphere has been neutralized. Such outflow ("shortcut") practically takes place in the first third of face length. Injected nitrogen can not reach even the danger zone [2,6] in the vicinity of gob balance line. Another inefficiency of large volume injecting is related to the ejection phenomenon involved in outflow of high-velocity jet. Area expansion of the nitrogen jet (fig.6), semi-restricted by the intake gate pillar ($y=0$ on fig.1) ends at 15 to 80 injector diameters in flow direction. Considering flow filtration nature and the relationship between environment porosity ε and extracted seam thickness, we believe that seam thickness is the more important factor. In relation to seam thickness, jet decomposition takes place at 0,55.m 2,93.m, where "m" is extracted seam thickness.

Semi-restricted nitrogen jet in the porous gob environment (fig.8) disintegrates a lot faster than a similar jet in free air and in main flow [6]. On the other hand, the jet disintegrates less but slower in non-uniform environment than in uniform one ($d_e = \text{const}$ and $\varepsilon = \text{const}$). This can be explained by naturally varying characteristics of porous environment presented in the flow model by α_{xy} and β_{xy} . In the expansion zone, filtration resistance is increasing faster crosswise than longitudinally that is why the expansion (fig.6) takes place significantly slower than in uniform porous environment. This is the reason why the jet disintegrates more slowly in natural non-uniformity. Velocity profiles on fig. 5 show displacement of maximal velocity from 0.1m to 2m from restricting pillar. At jet flow end, velocity is approximately 1 cm/s, i.e. significantly higher than undisturbed main flow velocity in the same profile.

With increase of initial nitrogen outflow velocity, the rate of maximal velocity reduction also increases (fig.7). The graph clearly show the impact of viscous and inertia losses in porous environment on these changes. Maximum velocity reduction shown on the figures, is almost linear for small quantities $Q_N=600 \text{ m}^3/\text{h}$ and $Q_N=900 \text{ m}^3/\text{h}$ and parabolic at $Q_N=3000 \text{ m}^3/\text{h}$. The curves on the figures follow from numerical modeling without additional approximation. Deeper into the gob ($x_0 \uparrow$) maximal velocity $U_m(x)$ reduction rate slows down (fig.7). Gob compaction, through change of ε , increases α_{xy} and β_{xy} . This leads to increase in outflow velocity but also to significantly greater pressure losses in flow direction. As a result, maximal velocity reduction rate $\left(\frac{dU_m}{dx}\right)$ slows down (fig.7).

With injected quantity increased, jet expansion angle decreases (fig.6). However, velocity gradient increases, between jet and main flow in the hydrodynamic boundary layer. This is one precondition for jet ejection factor increase.

With injector lagging behind face retreat ($x_0 \uparrow$), gob resistance increases ($\alpha_{xy} \uparrow, \beta_{xy} \uparrow$) behind outflow point ($x > x_0$). Additional ejection of air from nitrogen jet, due to increase of outflow velocity, is an adverse effect, which, in

addition to causing inert substance concentration decrease, also slows down main filtration flow outside jet distribution zone ($x \in 0 \dots B$). As a result, in the adjacent zone ($B < x < 0.5L_f$), heat exchange conditions favoring sponcom become significantly better.[6].

CONCLUSIONS AND RECOMMENDATIONS

Advantages and weak points of employed injection method.

Injection method – through a single pipe left in the gob at a height of 1 m above floor, has the following advantages:

- ⇒ In jet influence zone, oxygen concentration remains low thus preventing and suppressing coal oxidation;
- ⇒ The jet provides convective cooling to coal due to temperature gradient and high outflow velocity;
- ⇒ high outflow velocity ensures deeper penetration of nitrogen along gob contour, which is very important because of the coal left in pillars until first roof break;
- ⇒ simple injecting equipment.

The major weak points of conventional injection method, borrowed from Charbonnage de France, are as follows:

- ⇒ air ejection from the N-jet has adverse effect on injection both near the face and in gob depth;
- ⇒ nitrogen backflow during injection near the face (small x_0) in large quantities (Q_N);
- ⇒ high-velocity nitrogen outflow (w_{10}) leads to excessive coal drying in the jet influence zone. It could be assumed that such drying causes micro-fissures and additional structural damage of coal;
- ⇒ jet zone covers a too small portion (2-6%) of gob area, making jet suppression of sponcom fires with increased nitrogen quantities Q_N non- cost effective. Attempts for nitrogen quantity increase become ridiculous where coal is left throughout the entire gob area and particularly where $y < 1/3L_f$ - i.e. 1/3 of face length adjacent to intake gate;
- ⇒ it becomes inherently impossible to discontinue nitrogen injection without undertaking any other fire prevention measures. Any termination of nitrogen injection impacts negatively jet influence zone wherein:

the temperature rises most

convective heat transfer radically worsens because of manifold reduction of velocity and temperature gradient; coal is most dried up thus shortening the sponcom time- the stage of moisture evaporation[8] is missed.

Lack of theoretical and field research on nitrogen distribution is the reason why in recent year inertization has been thought a panacea for oxidation process suppression. Though such thinking has been refuted many times, it still exists in Babino Mine. Increase of nitrogen injection, even to hazardous quantities leading to oxygen deficiency in the face, has caused more than once isolation of mining areas rather than prevention of sponcom.

Efficient change of nitrogen injection mode.

Not all weak point can be avoided. Some of those are inherent to nitrogen injection method. Others, however, can be minimized and even avoided as shown in [6] and

evidenced by the results from numerical experiments of jet distribution.

First, it is necessary to reduce initial nitrogen outflow velocity w_{10} . This can be accomplished by:

⇒ injection through several pipes (increase of jet number).
The issues of pipe rotation has also been analyzed as alternative;

⇒ linear distribution of outflow;

⇒ area distribution of outflow;

Possible technology solutions are merit listed in [6]. A variant was selected based on comparative analysis, theoretical and practical considerations. Possibilities were also taken into account of combined application of other methods for sponcom prevention and suppression. On the basis of such analysis, in [6] an injector configuration is proposed along intake road. The proposed configuration ensures outflow velocity w_{10} decrease via splitting nitrogen quantity Q_N into three jets and locating outflows along height (z) and length (x_0). This in turn ensures three-phase increase of gradient (u_{10} - u_{20}) between jet and main flows with sufficient horizontal and vertical spacing of injector holes for more uniform velocity. Three-phase injection is an important precondition for reducing jet and main flow mixing distance. Hole location promotes three-phase static pressure increase, this pressure being the highest at the most remote injector from caving line. This injector is subjected to load from previous two pressure phases thus preventing air injection from face junction ($x=0, y=0$) with air intake gate.

Moreover, injection zone processing should be mandatory prior to and after injection. Prior to injection, foam pulp may be applied, and after injection - foaming substances' injection or flooding with pulp depending on gob incline in the pillar area and injection depth. The opportunity for more efficient foam pulp and pulp injection is an important advantage of three-point nitrogen injection.

Changes in nitrogen injection mode are necessary in terms of injection start point and quantity. Our research shows that injection at $x_0 < 15m$ is inadmissible, and at $x_0 = 20m$ - undesirable of quantities $Q_N > 1200m^3/h$.

The model allows optimization of nitrogen injection parameters in the jet flow zone. Model solution is applied successfully for specifying boundary and initial conditions in the nitrogen flow distribution model in the main air leakage flow [2], the latter model supplementing the nitrogen inertization picture for the entire gob area.

DENOTATIONS

$$A_{11} = \varphi_{10} \qquad A_{12} = -\bar{u}_2$$

$$A_{13} = \bar{b}_0 + (1 - k_1 x_0)(1 - b_0)m - \bar{u}_2$$

$$A_{21}(1 + \beta_x)\varphi_{11} \qquad A_{22} = \frac{\alpha_x \varphi_{10} v}{u_{10}}$$

$$A_{25} = \bar{b}_0 + (1 - k_1 x_0)(1 - b_0)m^2 - 0.64 \bar{u}_2^2 - \tau_o \bar{x}$$

$$A_{23} = -\varphi_{p1} \qquad A_{24} = -0.64 \bar{u}_2^2$$

$$A_{31} = \varphi_{12} \qquad A_{32} = 2 \varphi_{21} \alpha \qquad A_{33} = 2 \frac{v}{u_{10}} \varphi_{22}$$

$$A_{34} = \varphi_{11} \frac{v \alpha_x}{u_{10}} \qquad A_{35} = \varphi_{12} \beta_x$$

$$A_{41} = \frac{1}{\varphi_x} \bar{b}_0 \frac{\rho_a}{\rho_g}$$

$$\varphi_{10} = \int_0^1 f_1 d\xi = 0.795 \quad \varphi_{11} = \int_0^1 f_1^2 d\xi = 0.560 \quad \varphi_{12} = \int_0^1 f_1^3 d\xi = 0.565$$

$$\varphi_{21} = \int_0^1 f_1 f_p d\xi = 0.450$$

$$\varphi_{22} = \int_0^1 \left[\frac{\partial}{\partial \xi} (f_1) \right]^2 d\xi = -0.738 \quad \varphi_p = \int_0^1 f_p d\xi = 0.500$$

$$\varphi_N = \int_0^1 f_1 \sqrt{f} d\xi = 0.524 \quad f = \left(1 - \xi^{\frac{3}{2}} \right)^2$$

$$\alpha_x = \begin{cases} 3a \ 0 \leq x_0 \leq 10 \Rightarrow \alpha_x = 2615938 \\ 3a \ x > 10 \Rightarrow \alpha_x = 1,57 \times 10^6 + 161132 \otimes x_0 - \\ - 3372,76 \otimes x_0^2 + 34,069 \otimes x_0^3 - 0,128 \otimes x_0^4 \end{cases}$$

$$\beta_x = \begin{cases} 3a \ 0 \leq x_0 \leq 10 \Rightarrow \beta_x = 895,4167 \\ 3a \ x_0 > 10 \Rightarrow \beta_x = 78,876 + 126,329 \otimes x_0 - \\ - 1,35163 \otimes x_0^2 + 0,0596 \otimes x_0^3 \end{cases}$$

$$\text{erf}(0.68\xi) = 0.7675\xi - 0.1183\xi^3 + 0.0164\xi^5$$

REFERENCES

Michaylov M., E. Vlasseva. Modeling of Methane Distribution in a Gob Area of Coal Face. Proceeding of 1st International Symposium of Mine Environmental Engineering, Turkey, July 1996.

Michaylov M., E. Vlasseva. Modelling of Gob Inertization with Nitrogen, 8th US Mine Ventilation Symposium, June 11-17 1999, Rolla Missouri.

Луицянский Л.Г. Механика жидкости и газа. М.Наука. 1987.

Маджирски В. Гидродинамика. София. Техника, 1995.

Michaylov M., E. Vlasseva. Моделиране на разпределението на метан в обрушеното пространство. Доклад 3.2 по дог.123-3 "Теоретични изследвания върху ендеогенната пожароопасност на обрушеното пространство". Архив НИС на МГУ, декември 1997.

Michaylov M., E. Vlasseva. Моделиране на разпространението на азот в обрушеното пространство-експерименти за определяне на благоприятното масто и режим на инжектиране. Доклад 3.3 по дог.123-3 "Теоретични изследвания върху ендеогенната пожаро-

опасност на обрушеното пространство". Архив НИС на МГУ, септември 1998.
Теория турбулентных струй. Под.ред. Абрамовича Г.Н. М.Наука, 1984.

Markov Chr., M. Michaylov, (1989), Study of Self-heating Liability of Coal Seams of Bobov Dol Coal Field. *NITI "Minproject" RI, v. XXVII.*

Recommended for publication by Department of Mine Ventilation and Occupational Safety, Faculty of Mining Technology